Materials Today Bio 23 (2023) 100819

Contents lists available at ScienceDirect

Materials Today Bio

journal homepage: www.journals.elsevier.com/materials-today-bio

Cartilage fragments combined with BMSCs-Derived exosomes can promote tendon-bone healing after ACL reconstruction

Chi Zhang [a,b,1], Chao Jiang [c,1], Jiale Jin [a,1], Pengfei Lei [a,***], Youzhi Cai [a,b,*], Yue Wang [c,**]

[a] Center for Sports Medicine, The First Affiliated Hospital, Zhejiang University School of Medicine, 79 Qingchun Road, Hangzhou, 310008, China
[b] Institute of Sports Medicine of Zhejiang University, 388 Yuhangtang Road, Hangzhou, 310030, China
[c] Spine Lab, Department of Orthopedic Surgery, The First Affiliated Hospital, Zhejiang University School of Medicine, Hangzhou, China

ARTICLE INFO

Keywords:
Cartilage fragments
BMSCs-derived exosomes
Tunnel widening
Tendon-bone healing
ACLR

ABSTRACT

Anterior cruciate ligament reconstruction (ACLR) often fails due to the inability of tendon-bone integration to regenerate normal tissues and formation of fibrous scar tissues in the tendon-bone interface. Cartilage fragments and exosomes derived from bone mesenchymal stromal cells (BMSCs-Exos) can enhance enthesis healing. Nevertheless, the effects on the tendon-bone healing of ACLR remain unknown. This study found that BMSCs-Exos can promote the proliferation of chondrocytes in cartilage fragments, and activated the expression of chondro-related genes SOX9 and Aggrecan. The optimal effect concentration was 10^{12} events/uL. Besides, BMSCs-Exos could significantly upregulated the expression of BMP7 and Smad5 in cartilage fragments, and further enhanced the expression of chondrogenic genes. Moreover, this study established a rat model of ACLR and implanted the BMSCs-Exos/cartilage fragment complex into the femoral bone tunnel. Results demonstrated that the mean diameters of the femoral bone tunnels were significantly smaller in the BE-CF group than those in the CF group ($p = 0.038$) and control group ($p = 0.007$) at 8 weeks after surgery. Besides, more new bone formation was observed in the femoral tunnels in the BE-CF group, as demonstrated by a larger BV/TV ratio based on the reconstructed CT scans. Histological results also revealed the regeneration of tendon-bone structures, especially fibrocartilage. Thus, these findings provide a promising result that BMSCs-Exos/cartilage fragment complex can prevent the enlargement of bone tunnel and promote tendon-bone healing after ACLR, which may have resulted from the regulation of the BMP7/Smad5 signaling axis.

1. Introduction

Anterior cruciate ligament reconstruction (ACLR) is a well-established approach for treating ACL ruptures. Nevertheless, approximately 5%–23% of ACLR cases are failed [1,2] in large part, which can be attributed to unsuccessful tendon-bone healing [3,4]. The tendon-bone integration is unable to regenerate normal tissues after ACLR. Instead, the tendon-bone junction usually is replaced with fibrous scar tissues, resulting in weakened biomechanics of the tendon-bone interface and eventually failed ACLR. Various strategies, such as platelet-rich plasma, cytokine, stem cells, and autologous bone marrow, have been proposed to promote tendon-bone healing after ACLR [5–8]. However, none has been proven to be clinically effective. An efficacious therapeutic strategy that can promote tendon-bone healing after ACLR is clinically demanded.

Recent studies suggested that cartilage fragments with chondrocyte-matrix structures could potentially enhance chondrogenesis [9]. Cells migrated from cartilage fragments have a high proliferative ability. Moreover, cartilage fragments contain abundant stem cells, particularly cartilage-derived stem or progenitor cells (CSPCs), which have the potential to promote tendon-bone healing [10,11]. A study demonstrated that cartilage fragments could prevent femoral tunnel widening after

* Corresponding author. Center for Sports Medicine, the First Affiliated Hospital, Zhejiang University School of Medicine, 79 Qingchun Road, Hangzhou, 310008, China.
** Corresponding author. Spine Lab, Department of Orthopedic Surgery, the First Affiliated Hospital, Zhejiang University School of Medicine, 79 Qingchun Road, Hangzhou, 310008, China.
*** Corresponding author.
E-mail addresses: leipengfei@zju.edu.cn (P. Lei), caiyouzhi@zju.edu.cn (Y. Cai), wangyuespine@zju.edu.cn (Y. Wang).
[1] These authors contributed equally to this work.

https://doi.org/10.1016/j.mtbio.2023.100819
Received 19 April 2023; Received in revised form 11 September 2023; Accepted 23 September 2023
Available online 26 September 2023

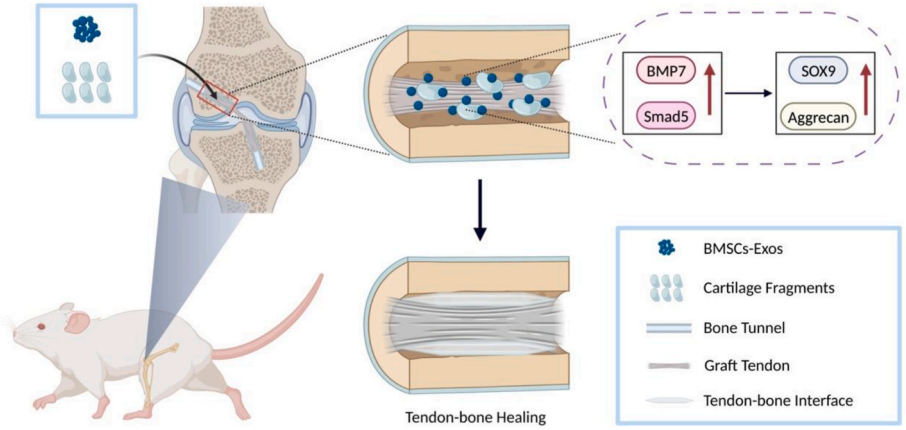

Scheme 1. Application of BMSCs-Exos/cartilage fragment complex for tendon-bone healing after ACLR.

ACLR [12] but could not regenerate sufficient cartilage tissues at the site of ACL insertion to achieve enthesis healing. Additional therapeutics are needed to promote tendon-bone healing in ACLR.

It is well-known that mesenchymal stem cells (MSCs) exert regenerative functions via paracrine, in which exosomes and membranous vesicles secreted by MSCs play a vital role in repairing [13]· Exosomes isolated from MSCs (MSCs-Exos) have similar biological characteristics to MSCs, which can deliver proteins and RNA to target cells to achieve regenerative effects [14,15]. In addition, MSCs-Exos are cell-free particles with lower immune responsiveness and higher stability than MSCs. Studies reported that MSCs-Exos could enhance chondrogenesis and tendon-bone healing, thus effectively treating cartilage defects and rotator cuff tear [16–18]. Furthermore, the fibrocartilaginous transition zone is a characteristic structure in the tendon-bone interface, and the regeneration of fibrous cartilage is a crucial step in tendon-bone formation [19,20]. In chondrogenesis, bone morphogenetic protein 7 (BMP7) is persistently upregulated during the formation of tendon-bone interface [21], and its downstream molecular Smad proteins play a vital role in regulating cartilage-related genes [22]. Given the evidence, the combination of MSCs-Exos and cartilage fragments may synergistically affect tendon-bone healing in ACLR via BMP7/Smad signaling.

Using a rat model of ACLR, this study combined cartilage fragments with BMSCs-Exos to promote tendon-bone healing. We hypothesized that the combination of cartilage fragments with BMSCs-Exos could prevent femoral tunnel widening, improve cartilage tissue generation and, thus, enable tendon-bone healing in ACLR. Further, this effect may be via the BMP7/Smad5 pathway (Scheme 1).

2. Materials and methods

2.1. Isolation, culture, and identification of cells

Two weeks-old Sprague-Dawley (SD) rats (100 ± 10 g) were used for CSPCs isolation, as previously described[13]. Knee joints were harvested from the rats, and cartilage tissues were separated. Cartilage tissues were cut into fragments using surgical scissors, then digested using 0.25% trypsin (Thermo, USA) and 300 units/mL of collagenase II (Thermo Fisher Scientific Life Sciences) solution at 37 °C for 8 h. The cell suspension was then filtered through a cell filter and centrifuged to concentrate the isolated chondrocytes. Primary chondrocytes were resuspended and inoculated on a plate coated with 10 μg/mL fibronectin (Sigma, USA) overnight at 4 °C. After culturing at 37 °C for 20 min, adherent cells were cultured in low-glucose Dulbecco's modified Eagle's medium (DMEM)/F12 1:1 medium (Sigma-Aldrich) supplemented with 10% (v/v) fetal bovine serum (FBS; Sigma-Aldrich), and 1% penicillin/streptomycin at 37 °C with 5% CO_2, and the medium was changed every other day. After being cultured for 12 days, the CSPCs colonies were newly formed. The positive or negative surface markers of CSPCs, including CD90, CD29, CD49e, CD73 and CD45, were detected with flow cytometry (Thermo, USA). The cells were cultured in corresponding mediums to examine osteogenic, adipogenic, and chondrogenic differentiation capacities. Each medium was changed every three days. The cells were fixed and stained with Alizarin Red S (for osteocytes), Oil Red O (for adipocytes), and Alcian Blue (for pellet culture chondrocytes) on day 14th (Leagene Biotechnology, China).

Bone Marrow Stromal Cells (BMSCs) were isolated from the femurs of 4-week-old SD rats. Bone marrow cells were cultured in DMEM supplemented with 10% FBS (Gibco, USA) at 37 °C cell incubator with 5% CO_2. We replaced the medium for the first time after 48 h and every three days afterward.

5-day-old rats were sacrificed, and the knee cartilage was extracted under the aseptic condition to prepare chondrocytes. Subsequently, the tissue was dissolved with 0.1% collagenase II for 6 h at 37 °C. Next, the digested cartilage tissues were suspended and seeded in culture dishes containing DMEM/F12 1:1 medium supplemented with 10% (v/v) FBS and 1% penicillin/streptomycin at 37 °C with 5% CO_2. The cells were passaged using 0.25% Trypsin-EDTA when they reached 80%–90% confluence. However, only P1 to P3 were used in this study.

2.2. Isolation and identification of BMSCs-Exos

BMSCs-Exos were isolated from the conditioned culture medium (CM) of BMSCs via super centrifugation. The main steps were as follows: 1) centrifuging CM at 300 g for 10 min to remove dead cells or cell fragments; 2) large microbubbles were removed by centrifugation at 20,000 g for 30 min; 3) the supernatant was transferred to a new test tube, and applied Poretics PCTE filter membrane of 0.8 μm, followed by ultra-high centrifugation (110,000 g centrifugation for 2 h) to concentrate and filter the sample. The concentrated sample was resuspended by PBS and centrifuged at 10^4 g for 1 h; 4) exosome particles were resuspended with 50–100 μL PBS and stored at −80 °C for subsequent experiments and identification.

Morphological characteristics of BMSCs-Exos were determined via transmission electron microscope (TEM) (JEM-1400, JEOL, Japan). Western blot was performed to confirm Exos markers, including Alix (Cell Signaling Technology, USA), TSG101 (Protein Tech, USA), and CD9 (Abcam, USA). The size distribution of BMSCs-Exos was determined using qNano analysis (Malvern, UK).

2.3. Internalization of BMSCs-Exos

The purified BMSCs-Exos were labeled with a lip-loving fluorescent PKH dye PKH-26 (Sigma-Aldrich, Germany). The PKH26-labeled BMSCs-Exos were then resuspended in the culture medium of CSPCs

and chondrocytes for 24 h. After fixation, the cells were washed with PBS three times, followed by immunostaining with QuickBlock buffer (Beyotime, China). The cytoskeleton was then stained with phalloidin (1:1000, Servicebio, China) for 120 min at room temperature and washed with PBS 3 times. Then, cells were stained with 4′, 6-diamino-2-phenylindole (DAPI; 1:1000, Solarbio, China) for 10 min and imaged by a confocal microscope (Olympus, Japan).

2.4. Cell viability assay

Cell viability assay of BMSCs-Exos was determined via a cell counting kit-8 (Beyotime, China). First, the CSPCs cells were transferred to 96-well plates and incubated with different concentrations (0, 10^8, 10^9, 10^{10}, 10^{11}, and 10^{12} events/uL) of BMSCs-Exos for 24 and 48 h. When the cells reached 90–95% confluence, the cells were washed with PBS, and 10 μL cell counting solution was added to the plate and incubated at room temperature for 2 h. The absorbance was measured at 450 nm with a microplate reader. All experiments were repeated three times.

2.5. Quantitative real-time PCR (qRT-PCR)

Total RNA was extracted from the cells via an RNA extraction kit (EZBioscience, USA) and digested with DNA enzymes to remove any contaminated genomic DNA as per the manufacturer's instructions. First-strand, the complementary DNA was synthesized (cDNA) via reverse transcription kit (Accurate Biology, China). The qRT-PCR was performed using FastStart Universal SYBR Green Master (Accurate Biology, China). The relative gene expression was calculated by 2-ΔΔCT method and normalized to GAPDH. All experiments were repeated in triplicate. Primer sequences were listed in Table S1.

2.6. Western blot analysis

Protein was extracted from cells by RIPA lysis buffer (Beyotime, China) with 1 mM phosphatase inhibitors (BOSTER, China) and phenylmethanesulfonyl fluoride (BOSTER, China). After examination of protein concentration via BCA protein assay kit (Beyotime, China), 50 μg of protein extract was separated by gel electrophoresis and then transferred to the polyvinylidene fluoride (Millipore, USA) membrane. After being blocked with StartingBlock (Thermo, USA) for 15min, the membranes were incubated with specific antibodies, including collagen II (1: 1000), Aggrecan (1: 1000), SOX-9 (1: 1000), and β-actin (1: 5000) overnight at 4 °C. After rinsing, the membranes were incubated with horseradish peroxidase-labeled secondary antibodies (Solarbio, China) for 2 h. After washing with TBST 3 times, the signals were visualized using the Image Lab 3.0 software.

2.7. siRNA construction and transduction

For siRNA examination, cells were transfected with BMP7-siRNA or only siRNA (negative control) using the LipofectamineTM RNAiMAX reagent according to the manufacturer's instructions. Rat BMP7-siRNA was designed and synthesized by Tsingke Biotechnology (Beijing, China).

BMP7-siRNA(5′-GCCGAGUUCAGGAUCUAUATT-3′ and 5′- UAUAGAUCCUGAACUCGGCTT-3′)

2.8. Lentivirus construction and transduction

Green fluorescent protein (GFP) only or the BMP-7 gene of replication-defective lentiviruses were used for the control (NC-OE) and target gene (BMP-7-OE) groups. Construction of the lentiviral vector encoding BMP-7-OE (LV-BMP-7-GFP) has been previously described. The lentivirus expressing BMP-7 was propagated and harvested using a virus packaging system (Tsingke Biotechnology, Beijing, China). The optimal multiplicity of infection for lentiviral infection of CPSCs was 40. BMP-7 expression was detected using western blot analysis.

2.9. Study design

Animal Care and Use Committee approved animal handling and experimental procedures in alignment with the National Institutes of Health Guide for the Care and Use of Laboratory Animals. A total of 60 male SD rats (aged 8–10 weeks; weight 250–300 g) underwent unilateral ACLR and were randomly assigned to 3 groups (20 rats in each group): (1) a control group in which rats underwent ACLR using autograft without implant; (2) a cartilage fragment (CF) group in which rats received ACLR using autograft with cartilage fragments placed in the femoral bone tunnel; (3) a BMSCs-Exos/cartilage fragment complex (BE-CF) group in which rats received ACLR using autograft with cartilage fragments placed in the femoral bone tunnel and an intratunnel injection of BMSCs-Exos. During 4 and 8 weeks after surgery, the bone tunnel was evaluated via micro-CT, and the tendon-bone healing was evaluated.

2.10. Surgical procedures

The rats were anesthetized using 5.0% chloral hydrate (intraperitoneal injection), ACLR was performed as follows: the flexor digitorum longus tendon, as an autograft, was harvested form the ipsilateral limb. After removing the muscle and fascia tissue attached to the surface of the tendon, the autograft was soaked in normal saline. A longitudinal incision was performed on the medial parapatellar to expose the knee joint, and then the ACL was full exposed and sectioned using a scalpel. After identified the footprints of ACL in tibial and femoral side, the surgeon using a 1.0 mm Kirschner wire to create femoral and tibial bone tunnels, and the autograft was shuttled through from the tibial bone tunnel to the femoral bone tunnel. The autograft was fixed with sutures tied over the periosteum at the tunnel outlets. Make sure the sutures were tight and then closed the wound layer by layer. In the CF group, cartilage specimen was harvested from the intercondylar notch or trochlear ridge, then was mechanically minced into approximately 0.5 mm^3 pieces. The fragments were placed between the femoral side of the graft and bone tunnel. In the BE-CF group, after settling the cartilage fragments as the CF group, intra-tunnel injections of BMSCs-Exos solution (0.2 mL) were performed using a 1 mL needle. After surgery, 800,000 units of penicillin was intramuscularly injected into each rat to prevent infection. All rats were allowed freely mobility in cages after surgery.

2.11. Histology and immunohistochemistry staining

Samples were embedded in paraffin and cut into consecutive 5 mm thick sections, which were perpendicular to the axis of the bone tunnel. Tissue sections were stained with H&E. Sections of the specimens were examined to assess the TBH interface under a light microscope (Leica). Then, TBH zone quality was analyzed using a modified histological scoring system, which is based on the presence of mature chondrocytes, the extent of fibrochondral tissue around the tendon, and the transition of the interface tissue from the bone to tendon. For immunohistochemical staining, Col2/SOX9/MMP13 antibody was incubated overnight at 4 °C, and then the second antibody was incubated for 1 h. Then, the tissue sections were stained with 3, 3-diaminobenzidine (DAB) substrates. The relative expression levels of Col2, SOX9 and MMP13 were quantitatively measured using *ImageJ* (version 1.53, National Institutes of Health, USA).

2.12. Micro-CT

Samples were scanned using a micro-computed tomography (μCT) system (Skyscan 1176, Kontich, Belgium) at a resolution of 9 μm at 50 kV (200 μA). NRecon (V1.6) and CTAn (V1.13.8.1) programs were used for image reconstruction. The region of interest (ROI) was defined as a continuous 30-slice of the medial subchondral bone of the tibia.

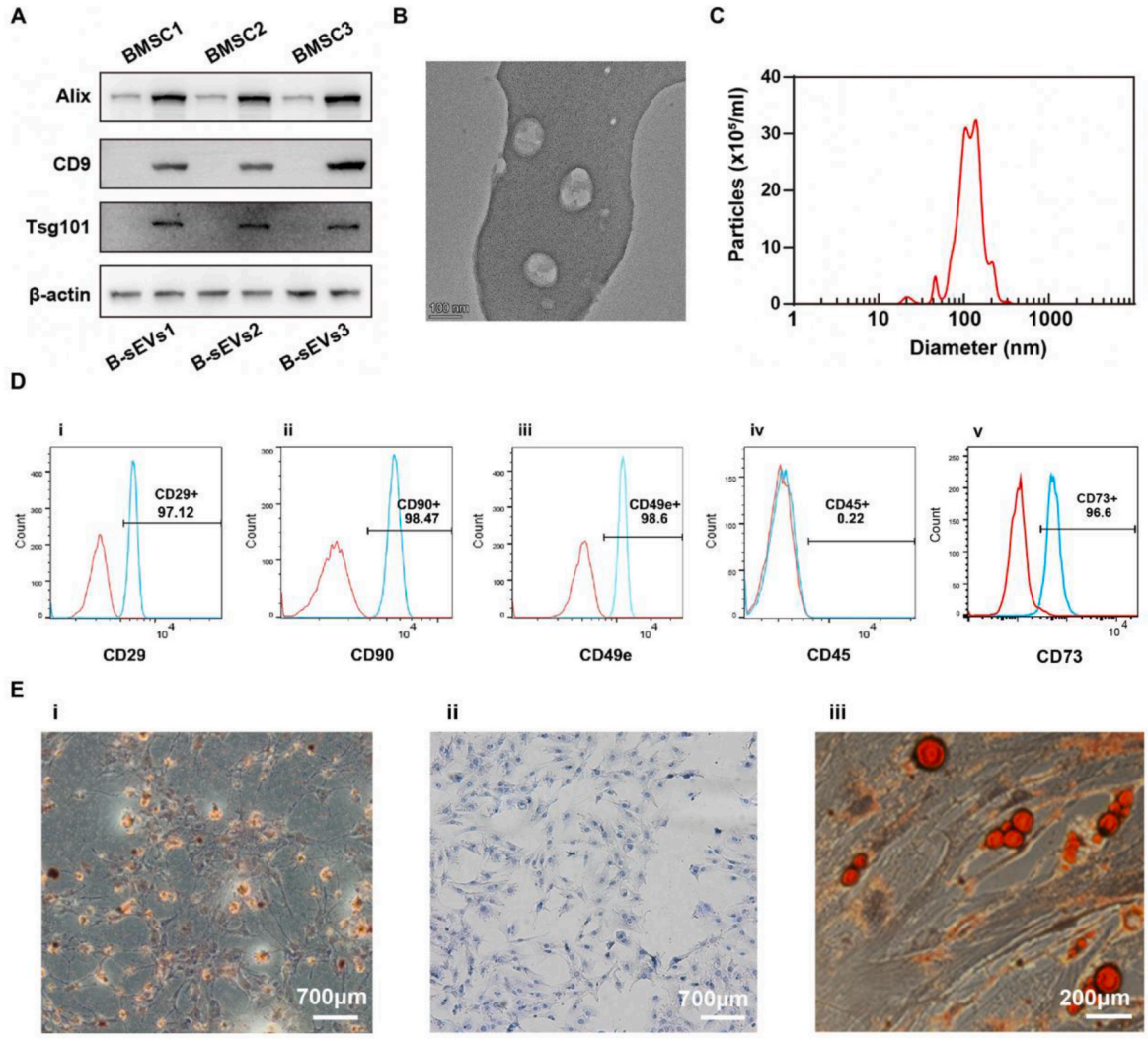

Fig. 1. Characterization and identification of BMSCs-Exos and CSPCs. (**A**) Western blot showed the presence of BMSCs-Exos specific markers CD9, Alix, and Tsg101. (**B**) BMSCs-Exos under a TEM. (**C**) qNano analysis revealed that the size of BMSCs-Exos ranged from 50 nm to 150 nm. (**D**) Flow cytometry showed positive or negative expression of surface markers CD90, CD29, CD49e, CD45 and CD34 for CSPCs. (**E**) Histology staining showed CSPCs have the ability of differentiating to osteoblast (i), chondrocyte (ii) and adipocyte (iii).

Subchondral bone specific parameters, including bone volume ratio (BV/TV, %), trabecular thickness (Tb.Th, mm), and trabecular separation (Tb.Sp., mm−1), were obtained for analysis.

2.13. Biomechanical testing

Biomechanical testing was performed using a tensile testing machine (Zwick/Roell Z020, German) with the distal edge of femur held in one vise grip of the testing instrument and with the proximal edge of tibia held in the other vise grip. The specimens were preloaded to 1 N and 10 cycles of preconditioning (elongation limits of 0–0.5 mm). After preconditioning, a pull-to-failure test with uniaxial tension at 10 mm/min was performed. Failure appeared as the presence of ruptured graft or pulling out of the tunnel, and the ultimate failure load was determined by the force to failure. Specimens were moistened with a saline solution during testing to avoid desiccation.

2.14. Statistical analysis

Statistical analysis was performed using STATA software (version 20.0, Chicago, USA), and data were presented as mean ± standard deviation (SD). One-way analysis of variance (ANOVA) with Bonferroni's *post hoc* tests was used to evaluate the significance of the experimental data. Non-parametric data were analyzed using the Kruskal-Wallis H test, and *p*-value less than 0.05 was considered statistically significant.

3. Results

3.1. Identification of BMSCs-Exos, and CSPCs

Exosome-specific markers, including CD9, Alix, and Tsg101 were examined using Western blot (Fig. 1A). BMSCs-Exos were circular particles with a size of 50–150 nm in qNano analysis under TEM (Fig. 1B and C). CD90, CD34, CD49e, CD29 and CD45 were used to detect CSPCs via flow cytometry (Fig. 1D). Besides, these cells can differentiate into osteoblast, chondrocyte, and adipocyte (Fig. 1E). Findings suggested that cartilage fragments contain massive CSPCs.

3.2. BMSCs-Exos promoted the proliferation and differentiation of CSPCs

BMSCs-Exos in the concentration of 0, 10^8, 10^9, 10^{10}, 10^{11}, and 10^{12} events/μL were added to the culture medium of CSPCs and chondrocyte to determine the optimal effect concentration of BMSCs-Exos on CSPCs and chondrocytes, respectively. Immunofluorescence showed that

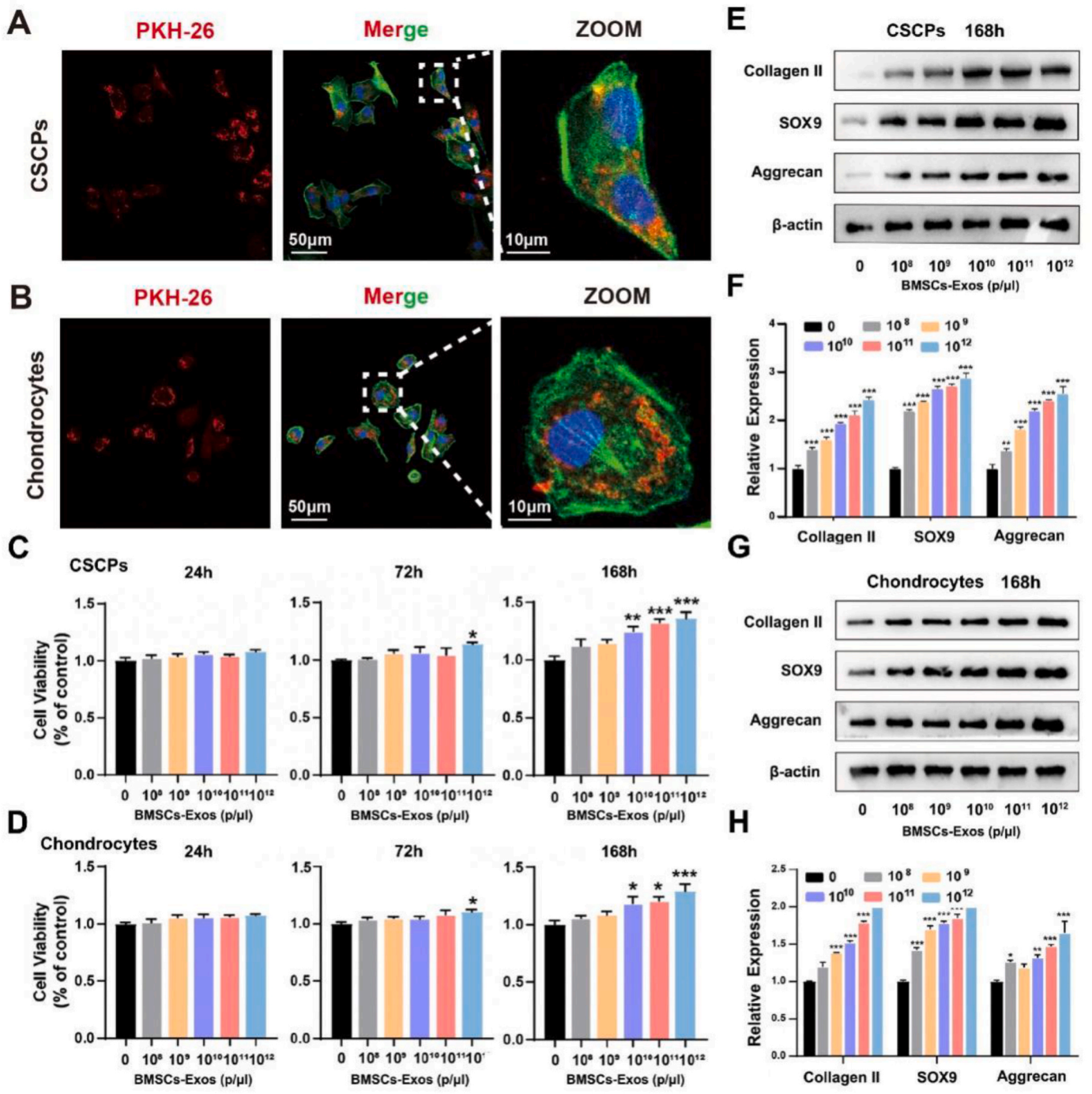

Fig. 2. Effects of different concentrations of BMSCs-Exos on the proliferation and differentiation of CSCPs and chondrocytes. (**A, B**) Immunofluorescence staining confirmed that CSCPs and chondrocytes phagocytosed BMSCs-Exos. (**C, D**) Effects of different concentrations of BMSCs-Exos (0, 10^9, 10^{10}, 10^{11} and 10^{12} events/μL) on the proliferation of CSCPs and chondrocytes. The expression of Collagen II, SOX9 and Aggrecan proteins (**E, G**) and genes (**F, H**) in CSCPs and chondrocytes treated with different concentrations of BMSCs-Exos. *, ** and *** indicate $p < 0.05$, $p < 0.01$ and $p < 0.001$, respectively.

BMSCs-Exos were successfully phagocytosed by the cells (Fig. 2A and B). CCK-8 assay revealed that 10^{12} events/μL BMSCs-Exos significantly promoted cell proliferation at 72 h. After culturing for 168 h, the proliferation of CSPCs and chondrocytes was enhanced in 10^9, 10^{10}, 10^{11}, and 10^{12} events/μL BMSCs-Exos. Notably, cell viability was increased significantly for both CSPCs and chondrocytes in 10^{12} events/μL BMSCs-Exos (Fig. 2C and D). In addition, BMSC-Exos in 10^{12} events/uL had the best capability to promote the differentiation of CSPCs to chondrocytes in Western blot, as compared with BMSC-Exos in other concentrations (Fig. 2E–H). As such, 10^{12} events/μL was selected as the optimal effect concentration for BMSCs-Exos and used in this study.

3.3. BMSCs-Exos upregulated BMP7 and Smad5 during chondrocyte differentiation

BMSCs and BMSCs-Exos with 10^{12} events/μL were added to cartilage fragments medium as treatments, respectively. After induction for 14 days, qRT-PCR results showed that the expression levels of BMP7, BMP2, Smad4, Smad5, and Runx2 were increased significantly during chondrogenesis in the BMSCs group. In the BMSCs-Exos group, the expression

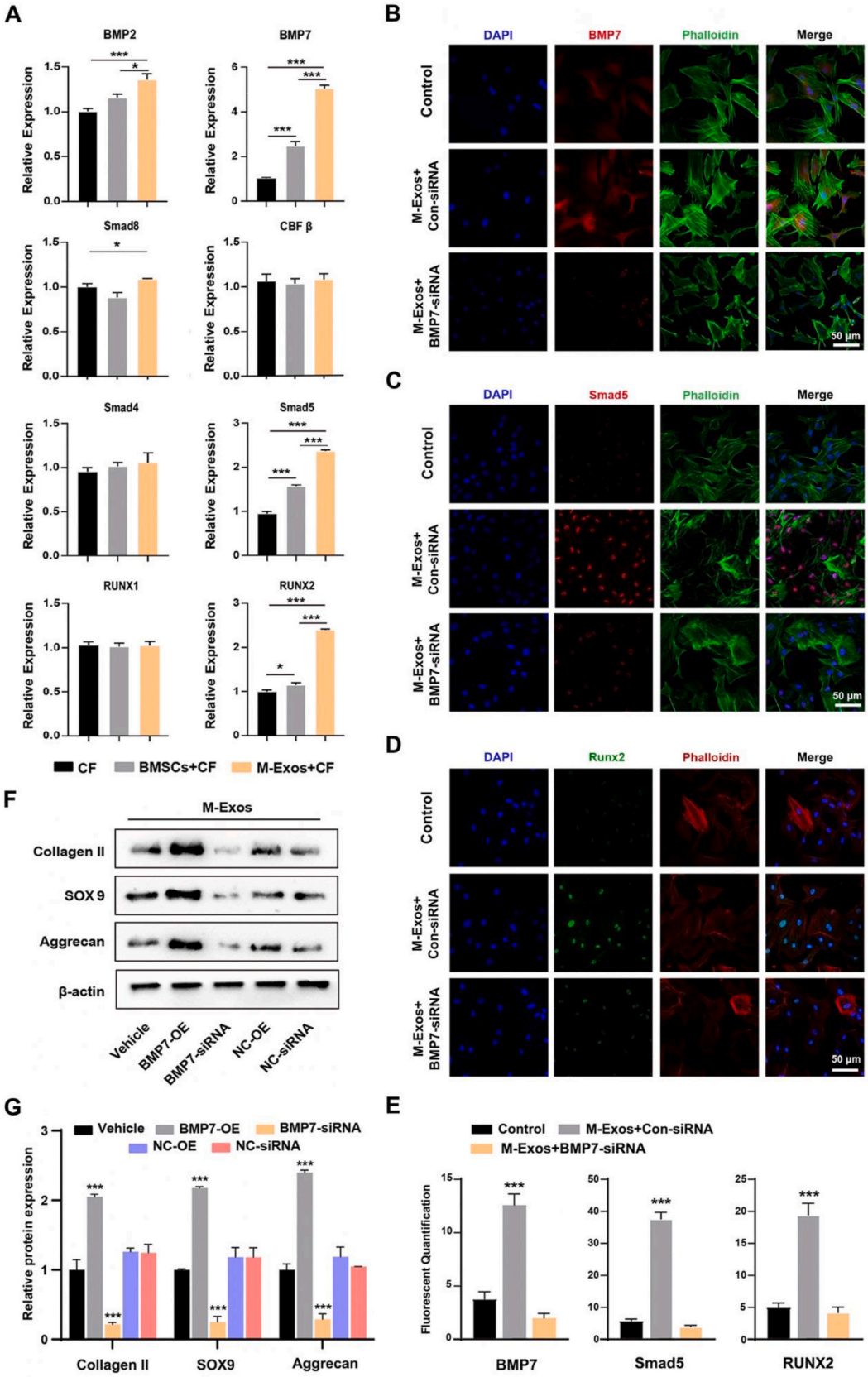

Fig. 3. Effects of BMSCs-Exos on chondrogenesis. (**A**) BMSCs-Exos induced mRNA expression of genes in chondrocytes. (**B, C, D**) Immunofluorescence images of BMP7, Smad5 and Runx2 proteins. (**E**) Quantification of BMP7, Smad5 and Runx2 flurescence. (**F**) Western blotting of proteins in chondrocytes combined with transfected CSCPs, which were induced by BMSCs-Exos. (**G**) Protein expression in chondrocytes, as assessed with semi-quantification. M-Exos, BMSCs-Exos; CF, cartilage fragment; OE, over expression; *, and *** indicate $p < 0.05$, and $p < 0.001$, respectively.

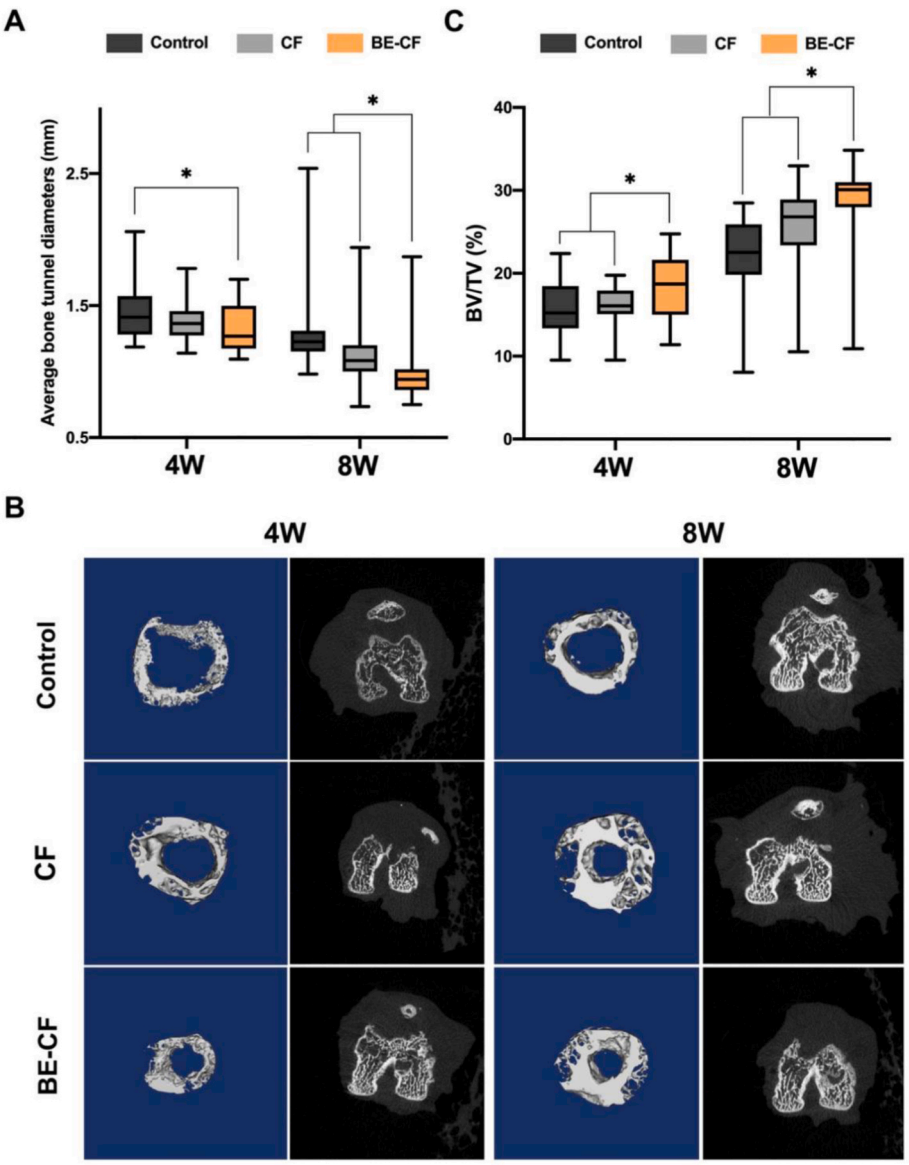

Fig. 4. Effects of BE-CF combination on bone tunnel in a rat model of ACLR. (**A**) The average diameter of the experimental femoral tunnel. (**B**) Reconstructed micro-CT images of the femoral tunnel 4 and 8 weeks after surgery. (**C**) The bone volume/total volume (BV/TV) ratios of the femoral tunnel in the control, CF and BE-CF groups. *: $p < 0.05$. CF: cartilage fragment; BE-CF: BMSCs-Exos and cartilage fragments complex.

levels of BMP7, Smad5, and Runx2 were increased and greater compared to the BMSCs group (Fig. 3A). Findings suggested that BMSCs-Exos can upregulate BMP7 and Smad5 expression *in vitro*.

3.4. BMSCs-Exos promoted cartilage formation via activating BMP7/Smad5 signaling

CSPCs isolated from cartilage fragments were harvested from SD rats' knees. Transfection was conducted to knock down the expression of BMP7. Transfected CSPCs were co-cultured with BMSCs-Exos in a chondrogenic medium. Immunofluorescence staining confirmed that the activity of BMP7 was decreased in the knockdown group but increased in the control group after being treated with BMSCs-Exos (Fig. 3B). Fluorescence intensity analysis demonstrated that the expression of BMP7 was significantly decreased in BMP7 knockdown group, even after BMSCs-Exos were added (Fig. 3E). Following chondrogenic induction for 14 days, the intensity of Smad5 and Runx2 staining was significantly decreased in the BMSCs-Exo + BMP7 knockdown group compared to other groups, as were in immunofluorescence staining and fluorescence intensity analysis (Fig. 3C, D, E). In addition, Western blot and qRT-PCR results showed that protein expression levels of cartilage-related genes, including Collagen II, SOX9, and Aggrecan, were significantly downregulated when BMP7 was knocked down in the BMSCs-Exos + BMP7-siRNA group. When BMP 7 was over-expressed, Collagen II, SOX9, and Aggrecan protein expression levels were upregulated significantly in the BMSCs-Exos + BMP7-OE group (Fig. 3F and G). Findings suggested that BMP7/Smad5 signaling may play a vital role in the BMSCs-Exos induced cartilage formation.

3.5. Cartilage fragments supplemented with BMSCs-Exos prevented tunnel widening and provided bioomechanical benefits after ACLR

In ACLR modeling, the femoral bone tunnel was drilled using a Kirschner wire (diameter 1.0 mm), which was used as the initial diameter of the tunnel. The femur bones were harvested and scanned with micro-CT from 4 to 8 weeks after surgery to measure the diameter of the femoral tunnel and BV/TV ratios (Fig. 4). The diameter of the femoral bone tunnel was 1.32 ± 0.18 mm in the BE-CF group is smaller than that

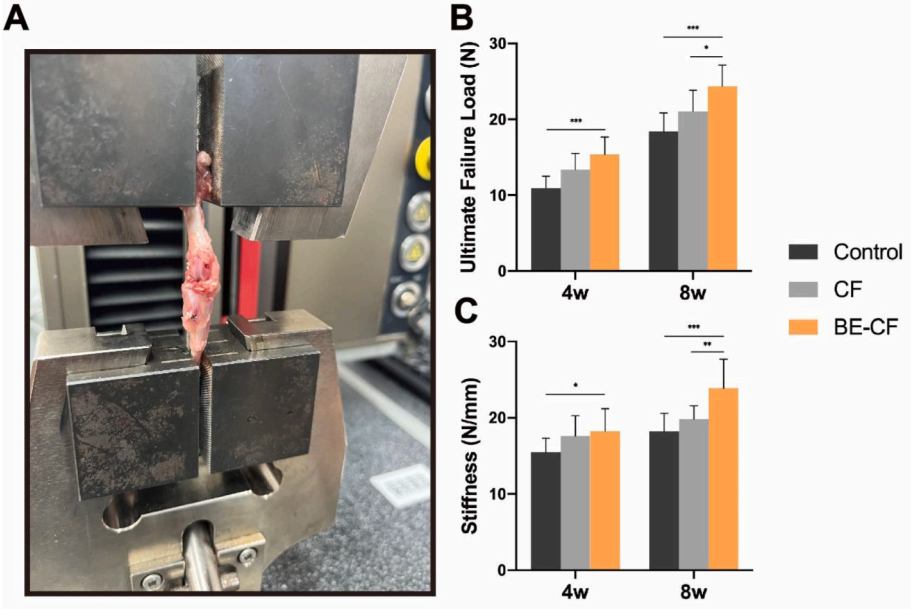

Fig. 5. Biomechanical testing. (**A**) An image of the procedure of biomechanical testing; (**B**) Comparison of ultimate failure load (N) in all three groups after 4 and 8weeks. (**C**) Comparison of stiffness (N/mm) in all three groups after 4 and 8weeks.*, and *** indicate $p < 0.05$, and $p < 0.001$, respectively.

in the control group (1.46± 0.23 mm, $p = 0.044$) at post-operative week 4. No significant difference in the tunnel diameter was observed between BE-CF and CF groups (1.32± 0.18 mm versus 1.38± 0.15 mm, $p = 0.326$). While, the diameter of femoral bone tunnel was significantly smaller in the BE-CF group (1.01± 0.26 mm) than in the CF group (1.15± 0.29 mm, $p = 0.01$) and control group (1.27± 0.32 mm, $p = 0.007$) after eight weeks (Fig. 4A). Moreover, more new bone was formed in the femoral tunnel in the BE-CF group compared to other groups at post-operative week 8 (Fig. 4B).

In addition, BV/TV ratio of the femoral tunnel (18.34 ± 4.08) was greater than the CF and control groups (16.05± 2.32, $p = 0.035$; 15.69± 3.26, $p = 0.029$, respectively) after four weeks. The BV/TV ratio of femoral tunnel (28.45± 5.96) in BE-CF group is greater than CF and control groups (25.25 ± 6.07, $p = 0.01$; 22.30± 4.55, $p = 0.001$, respectively) 8 weeks after surgery (Fig. 4C).

Biomechanical testing was used to detect the ultimate failure load after 4 and 8 weeks in all three groups (Fig. 5A). At 4 weeks after ACLR, a significantly higher failure load was recorded in BE-CF group (15.36 ± 2.31) in comparison with the control group (10.9 ± 1.56, $p < 0.0001$), but no difference was found in comparison with the CF group (13.37 ± 2.16, $p = 0.062$). And there was a significant difference in stiffness between the BE-CF group (18.24 ± 2.96) and the control group (15.47 ± 1.85, $p = 0.022$). While, at week 8, the ultimate failure load in BE-CF group (24.34 ± 2.83) was significantly higher than that in CF group (21.05 ± 2.78, $p = 0.018$) and control group (18.41 ± 2.45, $p < 0.0001$). Moreover, the BE-CF group exhibited a significant increase in stiffness (23.91 ± 3.8) compared with the CF group (19.82 ± 1.75, $p = 0.006$) and control group(18.21 ± 2.35,$p = 0.0008$)(Fig. 5B and C).

3.6. BMSCs-Exos combined with cartilage fragments promoted tendon-bone healing

Histological analysis was performed to assess the tendon-bone interface. In HE staining, pronounced chondrocytes and densely arranged collagen fibers were found between the graft and femoral bone tunnel in the BE-CF group at post-operative week 8. Besides, there was an apparent 'tidal line' structure in the tendon-bone interface. In the CF group, there were fewer chondrocytes in the interface compared to the BE-CF group, and no 'tidal line' structure was observed. In the control group, the interface between the graft and tunnel was surrounded by scar tissues with distributed chondrocytes (Fig. 6A). In immunohistochemical staining, there were more Aggrecan at the tendon-bone interface in rats treated with BE-CF than control and CF groups at both postoperative week 4 and 8 (Fig. 6B). In addition, immunofluorescence further revealed that there were significantly more BMP7 and SOX9 proteins at the interface in the BE-CF group than the other groups at 4 and 8 weeks after surgery. The results suggest that BE-CF promoted the expression of BMP7 and SOX9 *in vivo* (Fig. 6C–F).

4. Discussion

In this study, we found that BMSCs-Exos combined with cartilage fragments could enhance chondrogenesis via BMP7/Smad5 signaling axis *in vitro*. Furthermore, it could prevent femoral tunnel widening and promote tendon-bone healing in a rat model of ACLR.

It is generally accepted that better enthesis healing depends on increased ordered collagen fibers and new bone formation. Moreover, fewer scar tissues in the tendon-bone interface also improve enthesis healing [23,24]. After ACLR, many fibrous scar tissues formed (Sharpey fibers) between the graft and bone tunnel, resulting in tunnel widening [25]. Moreover, the disorganization of graft tendon is not conducive to tendon-one healing. The regeneration of fibrocartilage in the tendon-bone interface is essential in enthesis healing. Cartilage fragments have been induced for cartilage repair as a source of chondrocytes and CSPCs. Studies showed that chondrocytes and CSPCs are active on the surface of fragments and highly express proliferative markers such as β-catenin and cadherin. Besides, these markers have a strong proliferative ability, could migrate from the surface of the fragments [26–28], and are widely present in prechondrocytes. It is also involved in cell adhesion and signal transduction during chondrogenesis [29]. Different from growth factors, PRP and stem cells, chondrocytes outgrowing from cartilage fragments represent a unique subset with a proliferative phenotype that might promote a reliable fibrocartilage insertion of tendon-bone interface [30]. Besides, mature chondrocytes reserve stemness, which can generate chondrogenic progenitor cells for cartilage repair [10]. Our previous clinical study failed to produce expected outcomes on the possibility of cartilage fragments to prevent bone tunnel widening [12].

It is indicated that BMSCs-Exos could induce the expression of Aggrecan and SOX9 to promote chondrocyte proliferation, while

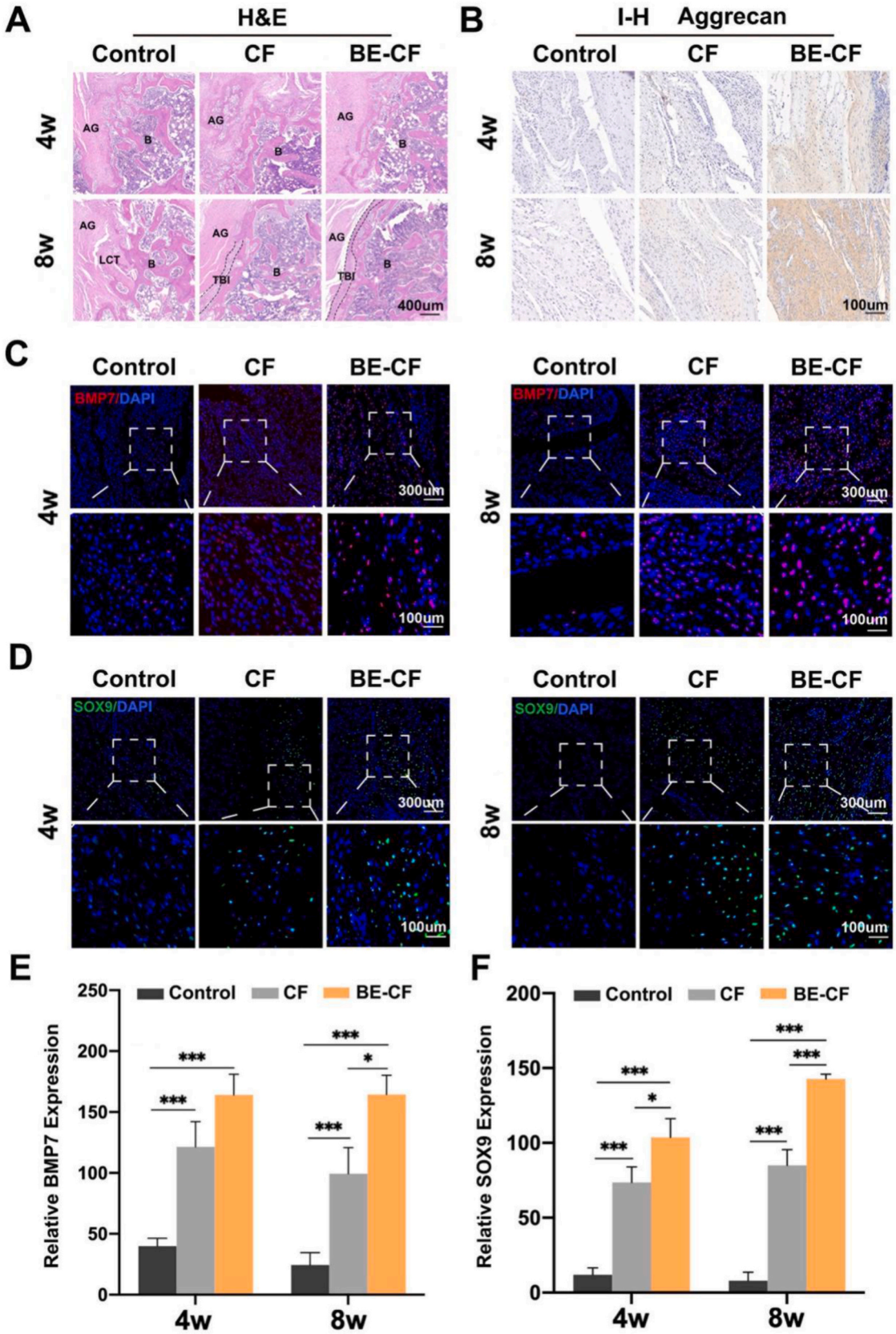

Fig. 6. Effects of BE-CF combination on tendon-bone healing in a rat model of ACLR. (**A**) Representative images of the graft-bone interface at postoperative week 4 and 8 (HE staining). **AG**, autograft; **B**, bone; **TBI**, tendon-bone interface; **LCT**, loose connective tissue. (**B**) Immunohistochemical staining for Aggrecan protein in the graft-bone interface 4 and 8 weeks after modelling. Immunofluorescence staining for BMP7 protein (**C**) and SOX9 protein (**D**) in the graft-bone interface at 4 and 8 weeks. Relative expression level for BMP7 (**E**) and SOX9 (**F**) in the graft-bone interface at 4 and 8 weeks. CF: cartilage fragment; BE-CF: BMSCs-Exos/cartilage fragments complex. * and *** indicate $p < 0.05$ and $p < 0.001$, respectively.

enhancing the expression of collagen-II and TGF-β1, reducing ADAMTS5 production and inhibiting inflammatory factors such as IL-1β and TNF-α from balancing the degradation and synthesis of extracellular matrix (ECM) [31–33]. Furthermore, chondrogenesis and ECM deposition are the essential processes during tendon-bone regeneration [34]. In this study, the application of BMSCs-Exos promoted the proliferation of chondrocytes migrated from cartilage fragments and further enhanced the expression of SOX9 and Aggrecan. Meanwhile, BMSCs-Exos also induced stem cells differentiation into cartilage cells. In vivo study further showed that the implantation of BMSCs-Exos/cartilage fragments complex in the femoral tunnel side after ACLR resulted in a significantly smaller tunnel diameter in the BE-CF group compared to other groups. Besides, micro-CT also indicated more new bone tissue formation in the tunnels of the BE-CF group than in the other groups. However, micro-CT can only be used to analysis differences in bone volume after repair, but can not resolute the microstructure of tendon-bone interface which is an important parameter in tendon-bone interface regeneration [35,36]. Thus, in further study, we should utilize a highly accurate method (μCT as previous reported strategies [37]) to directly visualize the tendon-bone interface regeneration after repairing. In addition, the view of tendon-bone interface was directly taken with a microscope, and showed that more fibrocartilage formation was observed at the tendon-bone interface in the BE-CF group than in the other groups. A specialized transition zone called 'tide line' between fibrocartilage and calcified cartilage layers was more pronounced in the BE-CF group. According to previous studies, new bone formation and fibrocartilage regeneration were essential for tendon-bone healing [38,39].

In addition, the possible mechanisms of BMSCs-Exos and cartilage fragments were investigated for tendon-bone healing. Previous studies have reported that during the formation of tendon-bone structure, the expression of BMP7 is significantly upregulated, which can induce stem cells to differentiate into osteoblasts and further improve the mechanical strength of tendon-bone interface [40,41]. Besides, BMP7 could also induce stem cells to differentiate into fibrocartilage for enhancing the regeneration of tendon-bone structure [42]. This study added BMSCs and BMSCs-Exos in cartilage fragments medium, respectively. It was found that BMP7 and Smad5 in the BE-CF group were upregulated, accompanied by a significant increase of SOX9 and Aggrecan expression higher than those in other groups. The expression of BMP7 was knocked down, followed by the expression of Smad5 and chondrogenic genes. In contrast, overexpression of BMP7 enhanced the expression of Smad5 and chondrogenic genes. These results showed that BMSCs-Exos might promote chondrogenic differentiation from cartilage fragments via the BMP7/Smad5 signaling axis. In addition, this study detected the histological properties and the biomechanical properties in the research. As previous studies reported [24], exosomes could increase stiffness and failure rate after ACLR. This study found new bone formation in the tunnel with high BV/TV ratios via micro-CT in BE-CF groups, Moreover, biomechanical experiments further demonstrated the therapeutic effect in the BE-CF group.

This study has some limitations. The healing process of SD rats is faster than humans. Thus, a large animal model must be used in further research to correlate with the healing period of humans. This experiment did not include the control group treated with BE alone to compare the effects of BE and BE-based therapies on tendon-bone healing.

5. Conclusion

This study demonstrated that BMSCs-Exos/cartilage fragment complex could prevent the enlargement of bone tunnel and promote tendon-bone healing after ACLR, which may have resulted from the regulation of the BMP7/Smad5 signaling axis. This study provides a new strategy for improving tendon-bone healing after ACLR, although further studies are required to confirm the effects for clinical application.

Credit author statement

All authors contributed to the article and approved the submitted version: Chi Zhang: Methodology, Investigation, Writing - Original Draft, Writing - Review & Editing. Chao Jiang: Methodology, Visualization, and Original Draft, Writing. Jiale Jin: Conceptualization, Writing - Review & Editing. Youzhi Cai: Conceptualization, Resources, Writing - Review & Editing, Supervision. Pengfei Lei: Conceptualization, Resources, Writing - Review & Editing. Yue Wang: Conceptualization, Writing - Review & Editing.

Declaration of competing interest

The authors declare the following financial interests/personal relationships which may be considered as potential competing interests: Chi Zhang reports financial support was provided by National Natural Science Foundation of China. Chi zhang reports financial support was provided by Natural Science Foundation of Zhejiang Province. Yue Wang reports financial support was provided by Science Technology Department of Zhejiang Province.

Data availability

Data will be made available on request.

Acknowledgements

This work was supported by National Natural Science Foundation of China (82002320, 82072398), and Natural Science Foundation of Zhejiang Province (LQ21H060005). We appreciate the technical support by Central laboratory, the First Affiliated Hospital, Zhejiang University School of Medicine.

Appendix A. Supplementary data

Supplementary data to this article can be found online at https://doi.org/10.1016/j.mtbio.2023.100819.

References

[1] R. Mascarenhas, B.J. Erickson, E.T. Sayegh, N.N. Verma, B.J. Cole, C. Bush-Joseph, B.R. Bach Jr., Is there a higher failure rate of allografts compared with autografts in anterior cruciate ligament reconstruction: a systematic review of overlapping meta-analyses, Arthroscopy 31 (2) (2015) 364–372, https://doi.org/10.1016/j.arthro.2014.07.011.

[2] M. Schmucker, J. Haraszuk, P. Holmich, K.W. Barfod, Graft failure, revision ACLR, and reoperation rates after ACLR with quadriceps tendon versus hamstring tendon autografts: a registry study with review of 475 patients, Am. J. Sports Med. 49 (8) (2021) 2136–2143, https://doi.org/10.1177/03635465211015172.

[3] B. Muller, K.F. Bowman Jr., A. Bedi, ACL graft healing and biologics, Clin. Sports Med. 32 (1) (2013) 93–109, https://doi.org/10.1016/j.csm.2012.08.010.

[4] M.E. Steiner, M.M. Murray, S.A. Rodeo, Strategies to improve anterior cruciate ligament healing and graft placement, Am. J. Sports Med. 36 (1) (2008) 176–189, https://doi.org/10.1177/0363546507311690.

[5] I. Andia, N. Maffulli, Biological therapies in regenerative sports medicine, Sports Med. 47 (5) (2017) 807–828, https://doi.org/10.1007/s40279-016-0620-z.

[6] A.L.L. de Andrade, A.V. Sardeli, T.A. Garcia, B. Livani, W.D. Belangero, PRP does not improve the objective outcomes of anterior cruciate ligament reconstruction: a systematic review and meta-analysis, Knee Surg. Sports Traumatol. Arthrosc. 29 (9) (2021) 3049–3058, https://doi.org/10.1007/s00167-020-06348-z.

[7] Z.C. Hao, S.Z. Wang, X.J. Zhang, J. Lu, Stem cell therapy: a promising biological strategy for tendon-bone healing after anterior cruciate ligament reconstruction, Cell Prolif. 49 (2) (2016) 154–162, https://doi.org/10.1111/cpr.12242.

[8] Y.S. Kim, C.H. Sung, S.H. Chung, S.J. Kwak, Y.G. Koh, Does an injection of adipose-derived mesenchymal stem cells loaded in fibrin glue influence rotator cuff repair outcomes? A clinical and magnetic resonance imaging study, Am. J. Sports Med. 45 (9) (2017) 2010–2018, https://doi.org/10.1177/0363546517702863.

[9] C. Zhang, Y.Z. Cai, X.J. Lin, One-step cartilage repair technique as a next generation of cell therapy for cartilage defects: biological characteristics, preclinical application, surgical techniques, and clinical developments, Arthroscopy 32 (7) (2016) 1444–1450, https://doi.org/10.1016/j.arthro.2016.01.061.

[10] Y. Jiang, Y. Cai, W. Zhang, Z. Yin, C. Hu, T. Tong, P. Lu, S. Zhang, D. Neculai, R. S. Tuan, H.W. Ouyang, Human cartilage-derived progenitor cells from committed

chondrocytes for efficient cartilage repair and regeneration, Stem Cells Transl. Med. 5 (6) (2016) 733–744, https://doi.org/10.5966/sctm.2015-0192.
[11] A. Marmotti, D.E. Bonasia, M. Bruzzone, R. Rossi, F. Castoldi, G. Collo, C. Realmuto, C. Tarella, G.M. Peretti, Human cartilage fragments in a composite scaffold for single-stage cartilage repair: an in vitro study of the chondrocyte migration and the influence of TGF-beta1 and G-CSF, Knee Surg. Sports Traumatol. Arthrosc. 21 (8) (2013) 1819–1833, https://doi.org/10.1007/s00167-012-2244-7.
[12] C. Zhang, J. Pan, J.D. Chen, Y.J. Zhang, P.C. Gu, X.J. Lin, Y.Z. Cai, The effect of cartilage fragments on femoral tunnel widening after anterior cruciate ligament reconstruction: a prospective randomized controlled study, Arthroscopy 34 (7) (2018) 2218–2227, https://doi.org/10.1016/j.arthro.2018.03.011.
[13] A.K. Batsali, A. Georgopoulou, I. Mavroudi, A. Matheakakis, C.G. Pontikoglou, H. A. Papadaki, The role of bone marrow mesenchymal stem cell derived extracellular vesicles (MSC-EVs) in normal and abnormal hematopoiesis and their therapeutic potential, J. Clin. Med. 9 (3) (2020), https://doi.org/10.3390/jcm9030856.
[14] C.R. Harrell, N. Jovicic, V. Djonov, V. Volarevic, Therapeutic use of mesenchymal stem cell-derived exosomes: from basic science to clinics, Pharmaceutics 12 (5) (2020), https://doi.org/10.3390/pharmaceutics12050474.
[15] C. Wang, Y. Zhang, G. Zhang, W. Yu, Y. He, Adipose stem cell-derived exosomes ameliorate chronic rotator cuff tendinopathy by regulating macrophage polarization: from a mouse model to a study in human tissue, Am. J. Sports Med. 49 (9) (2021) 2321–2331, https://doi.org/10.1177/03635465211020010.
[16] L. Han, H. Liu, H. Fu, Y. Hu, W. Fang, J. Liu, Exosome-delivered BMP-2 and polyaspartic acid promotes tendon bone healing in rotator cuff tear via Smad/RUNX2 signaling pathway, Bioengineered 13 (1) (2022) 1459–1475, https://doi.org/10.1080/21655979.2021.2019871.
[17] Y. Huang, B. He, L. Wang, B. Yuan, H. Shu, F. Zhang, L. Sun, Bone marrow mesenchymal stem cell-derived exosomes promote rotator cuff tendon-bone healing by promoting angiogenesis and regulating M1 macrophages in rats, Stem Cell Res. Ther. 11 (1) (2020) 496, https://doi.org/10.1186/s13287-020-02005-x.
[18] X. Xu, Y. Liang, X. Li, K. Ouyang, M. Wang, T. Cao, W. Li, J. Liu, J. Xiong, B. Li, J. Xia, D. Wang, L. Duan, Exosome-mediated delivery of kartogenin for chondrogenesis of synovial fluid-derived mesenchymal stem cells and cartilage regeneration, Biomaterials 269 (2021), 120539, https://doi.org/10.1016/j.biomaterials.2020.120539.
[19] H. Lu, C. Chen, S. Xie, Y. Tang, J. Qu, Tendon healing in bone tunnel after human anterior cruciate ligament reconstruction: a systematic review of histological results, J. Knee Surg. 32 (5) (2019) 454–462, https://doi.org/10.1055/s-0038-1653964.
[20] S. Thomopoulos, G.M. Genin, L.M. Galatz, The development and morphogenesis of the tendon-to-bone insertion - what development can teach us about healing, J. Musculoskelet. Neuronal Interact. 10 (1) (2010) 35–45.
[21] J. Xu, , X.Q. E, N.X. Wang, M.N. Wang, H.X. Xie, Y.H. Cao, L.H. Sun, J. Tian, H. J. Chen, J.L. Yan, BMP7 enhances the effect of BMSCs on extracellular matrix remodeling in a rabbit model of intervertebral disc degeneration, FEBS J. 283 (9) (2016) 1689–1700, https://doi.org/10.1111/febs.13695.
[22] Y. Yu, J.P. Bliss, W.J. Bruce, W.R. Walsh, Bone morphogenetic proteins and Smad expression in ovine tendon-bone healing, Arthroscopy 23 (2) (2007) 205–210, https://doi.org/10.1016/j.arthro.2006.08.023.
[23] R. Ma, M. Schar, T. Chen, M. Sisto, J. Nguyen, C. Voigt, X.H. Deng, S.A. Rodeo, Effect of dynamic changes in anterior cruciate ligament in situ graft force on the biological healing response of the graft-tunnel interface, Am. J. Sports Med. 46 (4) (2018) 915–923, https://doi.org/10.1177/0363546517745624.
[24] J. Xu, Z. Ye, K. Han, T. Zheng, T. Zhang, S. Dong, J. Jiang, X. Yan, J. Cai, J. Zhao, Infrapatellar fat pad mesenchymal stromal cell-derived exosomes accelerate tendon-bone healing and intra-articular graft remodeling after anterior cruciate ligament reconstruction, Am. J. Sports Med. 50 (3) (2022) 662–673, https://doi.org/10.1177/03635465211072227.
[25] A. Silva, R. Sampaio, E. Pinto, Femoral tunnel enlargement after anatomic ACL reconstruction: a biological problem? Knee Surg. Sports Traumatol. Arthrosc. 18 (9) (2010) 1189–1194, https://doi.org/10.1007/s00167-010-1046-z.
[26] D.E. Bonasia, J.A. Martin, A. Marmotti, R.L. Amendola, J.A. Buckwalter, R. Rossi, D. Blonna, H.D.t. Adkisson, A. Amendola, Cocultures of adult and juvenile chondrocytes compared with adult and juvenile chondral fragments: in vitro matrix production, Am. J. Sports Med. 39 (11) (2011) 2355–2361, https://doi.org/10.1177/0363546511417172.
[27] Y. Lei, J. Peng, Z. Dai, Y. Liao, Q. Liu, J. Li, Y. Jiang, Articular cartilage fragmentation improves chondrocyte migration by upregulating membrane type 1 matrix metalloprotease, Cartilage 13 (2_suppl) (2021) 1054S–1063S, https://doi.org/10.1177/19476035211035435.
[28] Y. Tsuyuguchi, T. Nakasa, M. Ishikawa, S. Miyaki, R. Matsushita, M. Kanemitsu, N. Adachi, The benefit of minced cartilage over isolated chondrocytes in atelocollagen gel on chondrocyte proliferation and migration, Cartilage 12 (1) (2021) 93–101, https://doi.org/10.1177/1947603518805205.
[29] N. Taniguchi, B. Carames, Y. Kawakami, B.A. Amendt, S. Komiya, M. Lotz, Chromatin protein HMGB2 regulates articular cartilage surface maintenance via beta-catenin pathway, Proc. Natl. Acad. Sci. U. S. A. 106 (39) (2009) 16817–16822, https://doi.org/10.1073/pnas.0904414106.
[30] Y. Lu, S. Dhanaraj, Z. Wang, D.M. Bradley, S.M. Bowman, B.J. Cole, F. Binette, Minced cartilage without cell culture serves as an effective intraoperative cell source for cartilage repair, J. Orthop. Res. 24 (6) (2006) 1261–1270, https://doi.org/10.1002/jor.20135.
[31] S. Cosenza, M. Ruiz, K. Toupet, C. Jorgensen, D. Noel, Mesenchymal stem cells derived exosomes and microparticles protect cartilage and bone from degradation in osteoarthritis, Sci. Rep. 7 (1) (2017), 16214, https://doi.org/10.1038/s41598-017-15376-8.
[32] K. Jiang, T. Jiang, Y. Chen, X. Mao, Mesenchymal stem cell-derived exosomes modulate chondrocyte glutamine metabolism to alleviate osteoarthritis progression, Mediat. Inflamm. 2021 (2021), 2979124, https://doi.org/10.1155/2021/2979124.
[33] Y. Wang, D. Yu, Z. Liu, F. Zhou, J. Dai, B. Wu, J. Zhou, B.C. Heng, X.H. Zou, H. Ouyang, H. Liu, Exosomes from embryonic mesenchymal stem cells alleviate osteoarthritis through balancing synthesis and degradation of cartilage extracellular matrix, Stem Cell Res. Ther. 8 (1) (2017) 189, https://doi.org/10.1186/s13287-017-0632-0.
[34] P.L. Hays, S. Kawamura, X.H. Deng, E. Dagher, K. Mithoefer, L. Ying, S.A. Rodeo, The role of macrophages in early healing of a tendon graft in a bone tunnel, J. Bone Joint Surg. Am. 90 (3) (2008) 565–579, https://doi.org/10.2106/JBJS.F.00531.
[35] L. Rossetti, L.A. Kuntz, E. Kunold, J. Schock, K.W. Muller, H. Grabmayr, J. Stolberg-Stolberg, F. Pfeiffer, S.A. Sieber, R. Burgkart, A.R. Bausch, The microstructure and micromechanics of the tendon-bone insertion, Nat. Mater. 16 (6) (2017) 664–670, https://doi.org/10.1038/nmat4863.
[36] R. Yang, G. Li, C. Zhuang, P. Yu, T. Ye, Y. Zhang, P. Shang, J. Huang, M. Cai, L. Wang, W. Cui, L. Deng, Gradient bimetallic ion-based hydrogels for tissue microstructure reconstruction of tendon-to-bone insertion, Sci. Adv. 7 (26) (2021), https://doi.org/10.1126/sciadv.abg3816.
[37] L. Wang, T. Zhu, Y. Kang, J. Zhang, J. Du, H. Gao, S. Chen, J. Jiang, J. Zhao, Crimped nanofiber scaffold mimicking tendon-to-bone interface for fatty-infiltrated massive rotator cuff repair, Bioact. Mater. 16 (2022) 149–161, https://doi.org/10.1016/j.bioactmat.2022.01.031.
[38] Y. Sun, W. Chen, Y. Hao, X. Gu, X. Liu, J. Cai, S. Liu, J. Chen, S. Chen, Stem cell-conditioned medium promotes graft remodeling of midsubstance and intratunnel incorporation after anterior cruciate ligament reconstruction in a rat model, Am. J. Sports Med. 47 (10) (2019) 2327–2337, https://doi.org/10.1177/0363546519859324.
[39] J.C. Zong, R. Ma, H. Wang, G.T. Cong, A. Lebaschi, X.H. Deng, S.A. Rodeo, The effect of graft pretensioning on bone tunnel diameter and bone formation after anterior cruciate ligament reconstruction in a rat model: evaluation with micro-computed tomography, Am. J. Sports Med. 45 (6) (2017) 1349–1358, https://doi.org/10.1177/0363546516686967.
[40] S. Chubinskaya, M. Hurtig, D.C. Rueger, OP-1/BMP-7 in cartilage repair, Int. Orthop. 31 (6) (2007) 773–781, https://doi.org/10.1007/s00264-007-0423-9.
[41] J. Stove, B. Schneider-Wald, H.P. Scharf, M.L. Schwarz, Bone morphogenetic protein 7 (bmp-7) stimulates proteoglycan synthesis in human osteoarthritic chondrocytes in vitro, Biomed. Pharmacother. 60 (10) (2006) 639–643, https://doi.org/10.1016/j.biopha.2006.09.001.
[42] F. Klatte-Schulz, S. Pauly, M. Scheibel, S. Greiner, C. Gerhardt, J. Hartwig, G. Schmidmaier, B. Wildemann, Characteristics and stimulation potential with BMP-2 and BMP-7 of tenocyte-like cells isolated from the rotator cuff of female donors, PLoS One 8 (6) (2013), e67209, https://doi.org/10.1371/journal.pone.0067209.